Available at: http://publications.ictp.it IC/2010/053

United Nations Educational, Scientific and Cultural Organization
and
International Atomic Energy Agency
THE ABDUS SALAM INTERNATIONAL CENTRE FOR THEORETICAL PHYSICS

SHAPE CHANGING NONLOCAL MOLECULAR DEFORMATIONS IN A NEMATIC LIQUID CRYSTAL

L. Kavitha[1]
Department of Physics, Periyar University, Salem-636 011, India
and
The Abdus Salam International Centre for Theoretical Physics, Trieste, Italy,

M. Venkatesh
Department of Physics, Periyar University, Salem-636 011, India

and

D. Gopi
Department of Chemistry, Periyar University, Salem-636 011, India.

Abstract

The nature of nonlinear molecular deformations in a homeotropically aligned nematic liquid crystal(NLC) is presented. We start from the basic dynamical equation for the director axis of a NLC with elastic deformation mapped onto a integro-differential perturbed Nonlinear Schrödinger equation which includes the nonlocal term. By invoking the modified extended tangent hyperbolic function method aided with symbolic computation, we obtain a series of solitary wave solutions. Under the influence of the nonlocality induced by the reorientation nonlinearity due to fluctuations in the molecular orientation, the solitary wave exhibits shape changing property for different choices of parameters. This intriguing property, as a result of the relation between the coherence of the solitary deformation and the nonlocality, reveals a strong need for deeper understanding in the theory of self-localization in NLC systems.

MIRAMARE – TRIESTE
July 2010

[1]Junior Associate of ICTP. Corresponding author: louiskavitha@yahoo.co.in

1. Introduction

Nonlinear dynamics of liquid crystals has been a subject of intensive study for more than two decades [1-2]. Not surprisingly, in both basic and applied research solitons have been found to have important effects in the mechanical, hydrodynamical and thermal properties of these highly nonlinear liquid crystals and play an important role in the switching mechanism of some ferroelectric liquid crystal displays [3-5]. In a nematic liquid crystal (NLC), the molecules are considered as elongated rods which are positionally disordered but reveal a long-range orientational order. This property is described on a mesocopic level by a unit vector $\mathbf{n}(\mathbf{r})$, which is called director axis pointing in the direction of the average molecular alignment. Due to the absence of a permanent polarization in the nematic phase the director just indicates the orientation but it has neither head nor tail. However, director reorientation or molecular excitation in NLC systems takes place due to elastic deformations such as splay, twist and bend [6].

The nonlinearity due to reorientation effect in a nematic phase leads to numerous effects not observed in any other types of nonlinearity. The nonlinear behaviour leads to soliton and under suitable conditions solitary waves can exist in NLC which has been investigated extensively both from theoretical and experimental points of view [7-16]. Propagation of solitons in a uniform shearing nematics was first studied by Lin et al. [6] and Zhu experimentally confirmed the existence of solitary-like director wave excited by a mechanical method [7]. Magnetically induced solitary waves were found to evolve in a NLC which was first discovered by Helfrich [8] and later confirmed by Legar [9]. Further, Migler and Meyer reported the novel nonlinear dissipative dynamic patterns and observed several types of soliton structures in the case of NLC under the influence of a continuously rotating magnetic field [10]. In addition, external field effects, multisolitons and the relation between observed optical-interference patterns and the director reorientation have also been investigated [11]. Single solitons generated by pressure gradients in long and circular cells of nematics, respectively, have also been reported recently [12]. Recently Daniel et al. studied the director dynamics in a quasi-one-dimensional NLC under elastic deformations in the absence of an external field without imposing the one constant approximation [17-18]. The molecular deformation in terms of a rotational director axis field is found to exhibit localized behaviour in the form of pulse, hole and shock as well as solitons [19].

In the present paper, we assume that our liquid crystal system is contained in an extremely narrow container with homeotropic alignment of molecules and with strong surface anchoring at the boundaries as illustrated in Figure 1. In this case, the molecular field due to elastic energy is assumed to be parallel to the director axis, which necessarily involves splay and bend type deformations in addition to twist. We attempt to demonstrate the shape changing director dynamics by employing the modified extended tangent hyperbolic (METF) method to solve the associated dynamical equation and understand the nonlinear dynamics.

The plan of the paper is as follows. We construct the dynamical torque equation representing the director dynamics and recast the same as equivalent to a perturbed nonlocal nonlinear Schrödinger (NLS) equation using the space-curve mapping procedure. We solve the perturbed integro-differential NLS by means of a computerized symbolic computation and the METF method is employed to construct a series of solitary wave solutions. Finally, we conclude our results.

2. Director dynamics

Liquid crystals are anisotropic materials with an anisotropy axis with molecular orientation. At a given temperature, NLC molecules fluctuate around the mean direction defined by the director $\mathbf{n(r)}$. The distortion of the molecular alignment corresponds to the free energy density of NLC [20-23] given by

$$f = \frac{1}{2}\{K_1(\nabla\cdot\mathbf{n})^2 + K_2(\mathbf{n}\cdot(\nabla\mathbf{x}\mathbf{n}))^2 + K_3(\mathbf{n}\mathbf{x}(\nabla\mathbf{x}\mathbf{n}))^2\}, \tag{1}$$

where K_i represents elastic constants for three different basic cannonical deformations splay ($i = 1$), twist ($i = 2$) and bend ($i = 3$). These constants are phenomenological parameters which can be connected with the intermolecular interaction giving rise to the nematic phase. Usually $K_3 > K_1 > K_2$, but Eq. (1) is simplified by assuming the one-elastic constant approximation $K_3 \simeq K_1 \simeq K_2 = K$. We ignore spatial variations in the degree of orientational order and describe the NLC in terms of the director rather than the order parameter tensor. We also ignore the effects of flow and work in the one-elastic approximation. Under this approximation, the free energy density given in Eq. (1) takes the simple form

$$f = \frac{K}{2}\{(\nabla\cdot\mathbf{n})^{\mathbf{2}} + (\nabla\mathbf{x}\mathbf{n})^{\mathbf{2}}\}. \tag{2}$$

To obtain the equation of motion, it is necessary to describe the generalized thermodynamic force acting on the director. We note that the molecular field h_{el} corresponding to the pure elastic deformations using the Lagrange equation $h_i = -\frac{\partial f}{\partial \mathbf{n}_i} + \partial_j \frac{\partial f}{\partial \mathbf{g}_{i,j}}$, $i, j = x, y, z$ and $\mathbf{g}_{ij} = \partial_j \mathbf{n}_i$ satisfies $\tilde{h} = h - (h\cdot\mathbf{n})\mathbf{n}$ introduced by de Gennes [1]. The quantity $(h\cdot\mathbf{n})$ may be interpreted as the Lagrange multiplier associated with the constraint that $\mathbf{n}^2 = 1$ and the condition for equilibrium is that $\tilde{h} = 0$ or $\tilde{h} = (h\cdot\mathbf{n})\mathbf{n}$. Nematic liquid crystals are charge carrying fluids with long range, uniaxial orientation and molecular alignment giving rise to anisotropic, macroscopic properties. By virtue of the anisotropic properties of nematic liquid crystals, it is advantageous to study the dynamics of director axis $\mathbf{n(r)}$ instead of studying the dynamics of all the molecules. In the absence of flow, the director axis $\mathbf{n(r)}$ does not remain in the same position but fluctuates about the mean position which is mainly due to the thermodynamical force caused by elastic deformation in nematics in the form of splay, twist and bend. Away from the equilibrium in the absence of flow, the thermodynamic force is balanced by a viscous force and the dynamics of the director is

$$\gamma\frac{\partial\mathbf{n}}{\partial t} = \tilde{h}, \tag{3}$$

where γ is a viscosity coefficient. In our model, NLC is contained in an extremely narrow container with the two ends along x-axis open and infinite. We assume rigid homoeotropic anchoring at the boundary walls. This gives the equation of motion

$$\frac{\partial \mathbf{n}}{\partial t} = \frac{K}{\gamma}\Big[\nabla^{\mathbf{2}}\mathbf{n} + (\mathbf{n}\cdot\nabla^{\mathbf{2}}\mathbf{n})\mathbf{n}\Big]. \tag{4}$$

Having derived the equation of motion to represent the dynamics the task ahead is to solve Eq. (4) and to understand the underlying director oscillations. However, Eq. (4) is a highly nontrivial vector nonlinear partial differential equation and it is very difficult to solve it in its natural form. This difficulty can be overcome by rewriting Eq. (4) in a suitable equivalent representation before solving. Experience shows that this can be done by mapping the NLC onto a moving helical space curve [24] in E^3 using a procedure in differential geometry in which Eq. (4) can be mapped to one of the Nonlinear Schrödinger family of equations or to its perturbed version. We map the NLC at a given instant of time onto a moving helical space curve in E^3 and a local coordinate system $\mathbf{e}_i$, $(i = 1, 2, 3)$ is formed on the space curve by identifying the unit director axis $\mathbf{n}(x,t)$ with the tangent vector $\mathbf{e_1}(x,t)$ of the space curve and by defining the unit principal and binormal vector $\mathbf{e_2}(x,t)$ and $\mathbf{e_3}(x,t)$, respectively, in the usual way. The change in the orientation of the orthogonal trihedral $\mathbf{e}_i(x,t)$, $(i = 1, 2, 3)$ which defines the space curve uniquely within rigid motions is determined by the Serret-Frenet (S-F) equations [25-26]

$$\begin{pmatrix} \vec{\mathbf{e}}_{1x} \\ \vec{\mathbf{e}}_{2x} \\ \vec{\mathbf{e}}_{3x} \end{pmatrix} = \begin{pmatrix} 0 & \kappa & 0 \\ -\kappa & 0 & \tau \\ 0 & -\tau & 0 \end{pmatrix} \begin{pmatrix} \vec{\mathbf{e}}_1 \\ \vec{\mathbf{e}}_2 \\ \vec{\mathbf{e}}_3 \end{pmatrix}, \tag{5}$$

where $\kappa \equiv (\mathbf{e}_{1x}\mathbf{e}_{1x})^{\frac{1}{2}}$ and $\tau \equiv \frac{1}{\kappa^2}\mathbf{e}_1(\mathbf{e}_{1x} \wedge \mathbf{e}_{1xx})$ are the curvature and torsion of the space curve. In view of the above identification and upon using the S-F Eqs. (5) $\mathbf{e}_{it}$ can be found and the trihedral evolves as

$$\mathbf{e}_{it} = \mathbf{\Omega} \wedge \mathbf{e}_i, \quad \mathbf{\Omega} = \omega_1\mathbf{e}_1 + \omega_2\mathbf{e}_2 + \omega_3\mathbf{e}_3, \tag{6}$$

where $\omega_1 = \frac{1}{\kappa(2\tau\kappa_x + \kappa\tau_x)}$, $\omega_2 = -\kappa\tau$ and $\omega_3 = \kappa_x$. Here the suffices t and x represent partial derivatives with respect to t and x. The conditions for compatibility of S-F equations (5) of the trihedron given by

$$(\mathbf{e}_{ix})_t = (\mathbf{e}_{it})_x, \quad i = 1, 2, 3, \tag{7}$$

lead to the following evolution equations for curvature and torsion of the space curve

$$\frac{\gamma}{K}\kappa_t = \kappa_{xx} - \kappa\tau^2, \tag{8a}$$

$$\frac{\gamma}{K}\tau_t = \kappa\tau^2 + \left(\frac{1}{\kappa^2}(\kappa\tau^2)_x\right)_x. \tag{8b}$$

In order to identify the set of coupled equations (8) with a more standard nonlinear partial differential equation, we make the following complex transformation

$$\psi(x,t) = \frac{1}{2}\kappa(x,t)\exp\Big\{\mathrm{i}\textstyle\int_{-\infty}^{x}\tau(x',t)dx'\Big\}, \tag{9}$$

also with appropriate rescaling of time and spatial variable as $t \longrightarrow$-i$\frac{\mu^2 Kt}{\gamma}$ and $\psi \longrightarrow \mu\psi$, we obtain the following integro-differential Nonlinear Schrödinger equation

$$\mathrm{i}\psi_t + \psi_{xx} + 2|\psi|^2\psi + \mu\psi \int_{-\infty}^{x} (\psi^* \psi_{x'} - 3\psi\psi^*_{x'}) dx' = 0. \tag{10}$$

Eq. (10) is a perturbed nonlinear Schrödinger equation and represents the director dynamics of our NLC system. When $\mu = 0$, Eq. (10) reduces to well-known completely integrable cubic Nonlinear Schrödinger equation which possess N-soliton solutions. The high anisotropy of physical properties as well as the collective behaviour of nematic molecules lead to nonlinear behaviour of the system, thus leading to nonlinear oscillations of the director axis $\mathbf{n(r)}$ governed by solitons. It might by mentioned that Eq. (10) resembles the damped NLS discussed by Pereira and Stenflo [27] except for the nonlocal term. In Eq.(10), μ represents the strength of nonlocal nonlinearity arises especially due to the molecular deformations and director oscillations. This nonlocal nature often results from transport processes such as atom diffusion, heat transfer, drift of electric charges [28-29] and in this case it is induced by a long range molecular interactions in NLC, which exhibit orientational nonlinearity [30-32]. Spatial nonlocality of the nonlinear response is a generic property of a wide range of physical systems, which manifests itself in new and exciting properties of nonlinear waves. This nonlocality implies that the response of the NLC medium at a given point depends not only on the wave function at that point(as in local media), but also on the wave function in its vicinity. In various areas of applied nonlinear science, nonlocality plays a relevant role and radically affects the underlying physics. Some striking evidences are found in plasma physics [31], in Bose-Einstein condensates (BEC) [32], where contrary to the prediction of purely local nonlinear models, nonlocality may give rise to or prevent, the collapse of a wave. In nonlinear optics, particularly when dealing with self-localization and solitary waves, nonlocality is often associated to time-domain phenomena through a retarded response, spatially nonlocal effects have been associated to photorefractive and thermal or diffusive processes [33]. In this context, we would like to investigate the effect of nonlocal term on the solitary director oscillations by constructing an exact solution to Eq.(10) using computational algebraic methods. It is a standard feature of nonlinear systems that exact analytic solutions are possible only in exceptional cases. In order to obtain the nature of nonlinear excitations of the system under consideration, we are often forced to attempt approximation methods. More recently, searching for exact solutions of nonlinear problems has attracted a considerable amount of research work and series of solutions can be found using symbolic computation.

3. Shape changing solitary oscillations

Various powerful methods for obtaining solitary wave solutions have been proposed such as Hirota's bilinear method , Painlevé expansions, the Inverse Scattering Transform, homogeneous balance method, F-expansion method, and Jacobi-elliptic function method [34-38]. Recently tanh method [36] has been proposed to find the exact solutions to nonlinear evolution equations.

Later, Fan [37] has proposed an extended tanh-function method and obtained new travelling wave solution that cannot be obtained by tanh-function method. Most recently, El-Wakil [38] modified the extended tanh-function method and obtained some new exact solutions. We employ the modified extended tanh-function (METF) method to solve the equation of motion Eq. (10) which governs the dynamics of director oscillations with elastic deformations such as splay, twist and bend. For convenience we substitute $\psi = u + iv$, and assume $\psi(\xi)$, $\xi(x,t) = x - ct$ in Eq. (10) and c is the velocity of the travelling wave. Upon separating the real and imaginary parts of the resultant equation, we obtain the following set of ordinary differential equations

$$cv_\xi + u_{\xi\xi} + 2(u^3 + v^2 u) + \mu u R = 0, \tag{11a}$$

$$R_\xi + 2(vv_\xi - uu_\xi) = 0, \tag{11b}$$

$$-cu_\xi + v_{\xi\xi} + 2(u^2 v + v^3) + \mu v R = 0, \tag{11c}$$

$$4(u_\xi v - uv_\xi) = 0, \tag{11d}$$

where, $R_\xi = -2(vv_\xi - uu_\xi) + \mathrm{i}4(u_\xi v - uv_\xi)$. In order to attempt to solve the above set of equations we introduce the following ansatz

$$u(\xi) = a_0 + \sum_{i=1}^{l} (a_i \phi^i + b_i \phi^{-i}), \tag{12a}$$

$$v(\xi) = b_0 + \sum_{j=1}^{m} (c_j \phi^j + d_j \phi^{-j}), \tag{12b}$$

$$R(\xi) = c_0 + \sum_{k=1}^{n} (e_k \phi^k + f_k \phi^{-k}), \tag{12c}$$

$$\frac{d\phi}{d\psi} = b + \phi^2, \tag{12d}$$

where b is the parameter to be determined later. The parameters l, m and n can be found by inserting Eq. (12) into Eq. (11) and balancing the higher-order linear term with the nonlinear terms as $l = m = 1$ and $n = 2$. Upon substituting Eq. (12) into the ordinary differential equations Eq. (11), will yield a system of algebraic equations with respect to $a_i, b, b_i, c_j, d_j, e_k$ and f_k since all the coefficients of ϕ^i, ϕ^j and ϕ^k have to vanish. We are interested to solve the system of equations for many choices of parameters in the following two different cases.

Case(a)

In this case we choose the set of parameters a_1, c_1, e_1 and e_2 vanish in order to satisfy Eq. (12d) and with the aid of Mathematica, we get a system of algebraic equations for $a_0, b_0, b, b_1, c_0, d_1, f_1$ and f_2

$$\begin{aligned}
&-cd_1 b\phi^{-2} - cd_1 + 2b_1 b^2 \phi^{-3} + 2b_1 b\phi^{-1} + 2a_0^3 + 2b_1^3 \phi^{-3} + 6a_0 b_1^2 \phi^{-2} + 6a_0^2 b_1 \phi^{-1} \\
&+2a_0 b_0^2 + 2b_0^2 b_1 \phi^{-1} + 2a_0 d_1^2 \phi^{-2} + 2b_1 d_1^2 \phi^{-3} + 4a_0 b_0 d_1 \phi^{-1} + 4b_0 b_1 d_1 \phi^{-2} + \mu a_0 c_0 \\
&+\mu a_0 f_1 \phi^{-1} + \mu a_0 f_2 \phi^{-2} + \mu c_0 b_1 \phi^{-1} + \mu b_1 f_1 \phi^{-2} + \mu b_1 f_2 \phi^{-3} = 0,
\end{aligned} \tag{13}$$

$$-f_1 b\phi^{-2} - f_1 - 2f_2 b\phi^{-3} - 2f_2\phi^{-1} - 2a_0 b_1 b\phi^{-2} - 2a_0 b_1 - 2b_1^2 b\phi^{-3} - 2b_1^2\phi^{-1}$$
$$-2b_0 d_1 b\phi^{-2} - 2b_0 d_1 - 2d_1^2 b\phi^{-3} - 2d_1^2\phi^{-1} = 0, \tag{14}$$

$$cb_1 b\phi^{-2} + cb_1 + 2d_1 b^2\phi^{-3} + 2d_1 b\phi^{-1} + 2b_0^3 + 2d_1^3\phi^{-3} + 6b_0 d_1^2\phi^{-2} + 6b_0^2 d_1\phi^{-1}$$
$$+2a_0^2 b_0 + 2a_0^2 d_1\phi^{-1} + 2b_0 b_1^2\phi^{-2} + 2b_1^2 d_1\phi^{-3} + 4a_0 b_0 b_1\phi^{-1} + 4a_0 b_1 d_1\phi^{-2}$$
$$+\mu b_0 c_0 + \mu b_0 f_1\phi^{-1} + \mu b_0 f_2\phi^{-2} + \mu c_0 d_1\phi^{-1} + \mu d_1 f_1\phi^{-2} + \mu d_1 f_2\phi^{-3} = 0, \tag{15}$$

$$4(-b_0 b_1 b\phi^{-2} - b_0 b_1 + a_0 d_1 b\phi^{-2} + a_0 d_1) = 0. \tag{16}$$

Further solving the system of equations using symbolic computation, we can distinguish two types solutions for this case as follows

Solution (i)

We collect the coefficients for different powers of ϕ and again solving the same we obtain

$$b = \mu a_0^2 + \mu b_0^2 - 3a_0^2 - 3b_0^2 - \frac{1}{2}\mu c_0, \tag{17a}$$
$$b_1 = -b_0(\frac{2a_0^2 + 2b_0^2 + \mu c_0}{c}), \tag{17b}$$
$$d_1 = -b_0^2(\frac{2a_0^2 + 2b_0^2 + \mu c_0}{a_0 c}), \tag{17c}$$
$$f_1 = 2b_0(\frac{(2a_0^2 + 2b_0^2 + \mu c_0)(a_0^2 + b_0^2)}{a_0 c}), \tag{17d}$$
$$f_2 = -b_0^2(\frac{(2a_0^2 + 2b_0^2 + \mu c_0)^2(a_0^2 + b_0^2)}{a_0^2 c^2}). \tag{17e}$$

Also upon using Eqs. (17) into Eqs. (12), we elucidate

$$\begin{aligned}\psi(x,t) \;=\; & a_0 + \left\{\left(-b_0(\frac{2a_0^2 + 2b_0^2 + \mu c_0}{c})\right)\sqrt{\mu a_0^2 + \mu b_0^2 - 3a_0^2 - 3b_0^2 - \frac{1}{2}\mu c_0}\right. \\ & \left. tan\left(\sqrt{\mu a_0^2 + \mu b_0^2 - 3a_0^2 - 3b_0^2 - \frac{1}{2}\mu c_0}\ (x - ct)\right)\right\} \\ & + \mathrm{i}\left[b_0 + \left(-b_0^2(\frac{2a_0^2 + 2b_0^2 + \mu c_0}{a_0 c})\right)\sqrt{\mu a_0^2 + \mu b_0^2 - 3a_0^2 - 3b_0^2 - \frac{1}{2}\mu c_0}\right. \\ & \left. tan\left(\sqrt{\mu a_0^2 + \mu b_0^2 - 3a_0^2 - 3b_0^2 - \frac{1}{2}\mu c_0}\ (x - ct)\right)\right],\end{aligned} \tag{18}$$

$$
\begin{aligned}
R(x,t) &= c_0 + \left\{ 2b_0 (\frac{(2a_0^2+2b_0^2+\mu c_0)(a_0^2+b_0^2)}{a_0 c}) \sqrt{\mu a_0^2 + \mu b_0^2 - 3a_0^2 - 3b_0^2 - \frac{1}{2}\mu c_0} \right. \\
& \left. tan\left(\sqrt{\mu a_0^2 + \mu b_0^2 - 3a_0^2 - 3b_0^2 - \frac{1}{2}\mu c_0} \;\; (x-ct) \right) \right\} \\
& - \left\{ b_0^2 (\frac{(2a_0^2+2b_0^2+\mu c_0)^2(a_0^2+b_0^2)}{a_0^2 c^2}) \sqrt{\mu a_0^2 + \mu b_0^2 - 3a_0^2 - 3b_0^2 - \frac{1}{2}\mu c_0} \right. \\
& \left. tan\left(\sqrt{\mu a_0^2 + \mu b_0^2 - 3a_0^2 - 3b_0^2 - \frac{1}{2}\mu c_0} \;\; (x-ct) \right) \right\}. \qquad (19)
\end{aligned}
$$

Eqs. (18-19) represent the exact solitary wave solutions in the form of kink excitations for the dynamical equation governing the director fluctuations due to molecular reorientation in NLC. In Fig. (2a-2h), we have plotted the solutions $\psi(x,t)$ and $R(x,t)$ represented in Eq. (18,19) by choosing $a_0 = 0.001, b_0 = 0.01$ and $c_0 = c = 1$ for various values of the parameter μ which physically signifies the role of nonlinear nonlocal term. From the figures, it is evident that any increment in the degree of nonlocality ($\mu > 0$) enables the kink-like excitation to gradually change its shape from kink to anti-soliton as depicted in Fig. (2a-2d) and Fig. (2i-2l) from anti-kink to anti-soliton, a more localized coherent soliton exhibiting shape changing property. It should be noted from the corresponding contour plots that the excitations due to reorientation nonlinearity are trapped so that it is highly localized and intact. In the contour plots the brighter region represents the maximum amplitude and the darker region represents the minimum or zero amplitude of the soliton. A noteworthy characteristic of these solitons is the way their coherence varies with the nonlocality parameter μ. The properties of nonlocal spatial incoherent soliton solutions has been investigated in NLC cells and the effect of nonlocality on the coherence properties of this self-trapped states have been studied in detail. In the case of coherent nematicons, the optically induced index profile tends to be broader than the soliton intensity profile depending on the degree of nonlocality thus leading to long range interactions in NLC systems [39-40]. The effects of nonlocality on coherent solitons, modulational instability and soliton interactions have also been investigated for several types of nonlocal response function [41].

Solution (ii)

In a similar way, we compute another set of solutions for b, b_1, d_1, f_1, f_2 as follows

$$b = -\frac{1}{2}\mu c_0 + \mu a_0^2 + \mu b_0^2 - 3a_0^2 - 3b_0^2, \tag{20a}$$

$$b_1 = \frac{a_0^2 c(-\mu c_0 + 2\mu a_0^2 + 2\mu b_0^2 - 6a_0^2 - 6b_0^2)}{6b_0(-2b_0^2 - 2a_0^2 + \mu a_0^2 + \mu b_0^2)}, \tag{20b}$$

$$d_1 = \frac{a_0 c(\mu c_0 + 2\mu a_0^2 + 2\mu b_0^2 - 6a_0^2 - 6b_0^2)}{6(-2b_0^2 - 2a_0^2 + \mu a_0^2 + \mu b_0^2)}, \tag{20c}$$

$$f_1 = -\frac{1}{3}\frac{a_0 c(-\mu c_0 + 2\mu a_0^2 + 2\mu b_0^2 - 6a_0^2 - 6b_0^2)}{b_0(\mu - 2)}, \tag{20d}$$

$$f_2 = -\frac{1}{36}\frac{a_0^2 c^2(-\mu c_0 + 2\mu a_0^2 + 2\mu b_0^2 - 6a_0^2 - 6b_0^2)^2}{(\mu - 2)(-2b_0^2 - 2a_0^2 + \mu a_0^2 + \mu b_0^2)b_0^2}. \tag{20e}$$

Upon substituting Eqs. (20) in Eqs. (12), the solution takes the following form

$$\begin{aligned}\psi(x,t) \;=\; & a_0 + \Bigg\{\left(\frac{a_0^2 c(-\mu c_0 + 2\mu a_0^2 + 2\mu b_0^2 - 6a_0^2 - 6b_0^2)}{6b_0(-2b_0^2 - 2a_0^2 + \mu a_0^2 + \mu b_0^2)}\right) \\ & \sqrt{-\frac{1}{2}\mu c_0 + \mu a_0^2 + \mu b_0^2 - 3a_0^2 - 3b_0^2} \\ & tan\left(\sqrt{-\frac{1}{2}\mu c_0 + \mu a_0^2 + \mu b_0^2 - 3a_0^2 - 3b_0^2}\ \ (x - ct)\right)\Bigg\} \\ & +\mathrm{i}\Bigg[b_0 + \left(\frac{a_0 c(\mu c_0 + 2\mu a_0^2 + 2\mu b_0^2 - 6a_0^2 - 6b_0^2)}{6(-2b_0^2 - 2a_0^2 + \mu a_0^2 + \mu b_0^2)}\right) \\ & \sqrt{-\frac{1}{2}\mu c_0 + \mu a_0^2 + \mu b_0^2 - 3a_0^2 - 3b_0^2} \\ & tan\left(\sqrt{-\frac{1}{2}\mu c_0 + \mu a_0^2 + \mu b_0^2 - 3a_0^2 - 3b_0^2}\ \ (x - ct)\right)\Bigg],\end{aligned} \tag{21}$$

$$\begin{aligned}R(x,t) \;=\; & c_0 + \Bigg\{\left(\frac{-a_0 c(-\mu c_0 + 2\mu a_0^2 + 2\mu b_0^2 - 6a_0^2 - 6b_0^2)}{3b_0(\mu - 2)}\right) \\ & \sqrt{-\frac{1}{2}\mu c_0 + \mu a_0^2 + \mu b_0^2 - 3a_0^2 - 3b_0^2} \\ & tan\left(\sqrt{-\frac{1}{2}\mu c_0 + \mu a_0^2 + \mu b_0^2 - 3a_0^2 - 3b_0^2}\ \ (x - ct)\right)\Bigg\} \\ & -\Bigg\{\left(\frac{1}{36}\frac{a_0^2 c^2(-\mu c_0 + 2\mu a_0^2 + 2\mu b_0^2 - 6a_0^2 - 6b_0^2)^2}{(\mu - 2)(-2b_0^2 - 2a_0^2 + \mu a_0^2 + \mu b_0^2)b_0^2}\right) \\ & \sqrt{-\frac{1}{2}\mu c_0 + \mu a_0^2 + \mu b_0^2 - 3a_0^2 - 3b_0^2} \\ & tan\left(\sqrt{-\frac{1}{2}\mu c_0 + \mu a_0^2 + \mu b_0^2 - 3a_0^2 - 3b_0^2}\ \ (x - ct)\right)\Bigg\}.\end{aligned} \tag{22}$$

The above solitary solutions also exhibit shape changing property. We have plotted Eqs. (21-22) in Fig. (3a-3h) by choosing the parametric values $a_0 = b_0 = 0.01$ and $c_0 = c = 1$ and the corresponding contour plots are also depicted. The parameter μ can be considered as a measure of the nonlocality of this nonlinear medium which is also evident from Fig. (3). As portrayed in Fig. (3a-3d), for $\mu = 0.03$, the director fluctuations represented in Eq. (21) are governed by anti-kink soliton and when μ is increased further the localized excitations continuously changing its shape and when $\mu = 0.2$, it takes the form of a coherent profile of anti-soliton. The shape changing property is also evident from the contour plots and when $\mu = 0.2$ the diagonal black region representing the peak of the coherent profile. Similarly, from Fig. (3i-3n) for Eqs.(22), one can observe that how the molecular reorientational nonlinearity balances with the nonlocal parameter and settles up in the kink soliton periodic profile when $\mu = 1.9$.

Case(b)

In this case, the parameters b_1, d_1, f_1 and f_2 vanishes, on inserting Eq. (12) into Eq. (11) we get an algebraic set of equations as follows

$$\begin{aligned} &cc_1b + cc_1\phi^2 + 2a_1b\phi^1 + 2a_1\phi^3 + 2a_1^3\phi^3 + 2a_0^3 + 6a_0a_1^2\phi^2 + 6a_0^2a_1\phi^1 + 2a_0b_0^2 \\ &+2a_0c_1^2\phi^2 + 2a_0b_0c_1\phi^1 + 2a_1b_0^2\phi^1 + 2a_1c_1^2\phi^3 + 4a_1c_1b_0\phi^2 + \mu a_0c_0 + \mu a_0e_1\phi^1 \\ &+\mu a_0e_2\phi^2 + \mu a_1c_0\phi^1 + \mu a_1e_1\phi^2 + \mu a_1e_2\phi^3 = 0, \end{aligned} \tag{23}$$

$$\begin{aligned} &e_1b + e_1\phi^2 + 2e_2b\phi^1 + 2e_2\phi^3 + 4a_0a_1b\phi^1 + 4a_0a_1\phi^3 + 4a_1^2b\phi^2 + 4a_1^2\phi^4 + 4b_0c_1b\phi^1 \\ &+4b_0c_1\phi^3 + 4c_1^2b\phi^2 + 4c_1^2\phi^4 = 0, \end{aligned} \tag{24}$$

$$\begin{aligned} &-ca_1b - ca_1\phi^2 + 2c_1b\phi^1 + 2c_1\phi^3 + 2b_0^3 + 2c_1^3\phi^3 + 6b_0c_1^2\phi^2 + 3b_0^2c_1\phi^1 + 2a_0^2b_0 + 2a_1^2b_0\phi^2 \\ &+4a_0b_0a_1\phi^1 + 2a_0^2c_1\phi^1 + 2a_1^2c_1\phi^3 + 4a_0a_1c_1\phi^2 + \mu b_0c_0 + \mu b_0e_1\phi^1 + \mu b_0e_2\phi^2 \\ &+\mu c_0c_1\phi^1 + \mu c_1e_1\phi^2 + \mu e_2c_1\phi^3 = 0, \end{aligned} \tag{25}$$

$$4(a_1b_0b + b_0a_1\phi^2 - a_0c_1b - a_0c_1\phi^2) = 0. \tag{26}$$

Solving the system of equations with the aid of Mathematica, we find the two types of solutions for b, a_1, c_1, e_1 and e_2.

Solution (iii)

We collect the coefficients for different powers of ϕ and solving the same we obtain

$$b = -b_0\left(\frac{-6b_0^4 - 12a_0^2b_0^2 - \mu c_0 b_0^2 + 4\mu a_0^2 c_0 + \mu^2 c_0^2}{-c^2 b_0 + 2c\mu a_0^3 + 2cb_0^2 a_0 \mu + 4b_0^3 + 8b_0 a_0^2 + 2b_0 c_0 \mu}\right), \tag{27a}$$

$$a_1 = -\left(\frac{-c^2 b_0 + 2c\mu a_0^3 + 2cb_0^2 \mu a_0 + 4b_0^3 + 8b_0 a_0^2 + 2b_0 c_0 \mu}{c(-3b_0^2 + \mu c_0)}\right), \tag{27b}$$

$$c_1 = -b_0\left(\frac{-c^2 b_0 + 2c\mu a_0^3 + 2cb_0^2 \mu a_0 + 4b_0^3 + 8b_0 a_0^2 + 2b_0 c_0 \mu}{ca_0(-3b_0^2 + \mu c_0)}\right), \tag{27c}$$

$$\begin{aligned} e_1 = {} & \frac{24b_0^5 + 72b_0^3 a_0^2 + 12b_0^3 c_0 \mu + 12a_0^2 b_0 c_0 \mu - 3c^2 b_0^3 + 18b_0^2 ca_0^3 \mu - 6a_0^2 c^2 b_0}{ca_0(-3b_0^2 + \mu c_0)} \\ & + \frac{6b_0^4 a_0 c\mu + 12a_0^5 c\mu + 48a_0^4 b_0 - c^2 b_0 \mu c_0 + 2c\mu^2 a_0^3 c_0 + 2cb_0^2 \mu^2 a_0 c_0}{\mu ca_0(-3b_0^2 + \mu c_0)}, \end{aligned} \tag{27d}$$

$$e_2 = 2\frac{(-c^2 b_0 + 2c\mu a_0^3 + 2cb_0^2 \mu a_0 + 4b_0^3 + 8b_0 a_0^2 + 2b_0 c_0 \mu)(a_0^2 + b_0^2)}{ca_0(-3b_0^2 + \mu c_0)}. \tag{27e}$$

Also upon using Eqs. (27) into Eq. (12), we elucidate

$$\begin{aligned} \psi(x,t) = {} & a_0 - \left(\frac{-c^2 b_0 + 2c\mu a_0^3 + 2cb_0^2 \mu a_0 + 4b_0^3 + 8b_0 a_0^2 + 2b_0 c_0 \mu}{c(-3b_0^2 + \mu c_0)}\right) \\ & \sqrt{b_0 \frac{-6b_0^4 - 12a_0^2 b_0^2 - \mu c_0 b_0^2 + 4\mu a_0^2 c_0 + \mu^2 c_0^2}{-c^2 b_0 + 2c\mu a_0^3 + 2cb_0^2 a_0 \mu + 4b_0^3 + 8b_0 a_0^2 + 2b_0 c_0 \mu}} \\ & tanh\left(\sqrt{b_0 \frac{-6b_0^4 - 12a_0^2 b_0^2 - \mu c_0 b_0^2 + 4\mu a_0^2 c_0 + \mu^2 c_0^2}{-c^2 b_0 + 2c\mu a_0^3 + 2cb_0^2 a_0 \mu + 4b_0^3 + 8b_0 a_0^2 + 2b_0 c_0 \mu}}\ (x - ct)\right) \\ & + \mathrm{i}\left[b_0 - \left(b_0 \frac{(-c^2 b_0 + 2c\mu a_0^3 + 2cb_0^2 \mu a_0 + 4b_0^3 + 8b_0 a_0^2 + 2b_0 c_0 \mu)}{ca_0(-3b_0^2 + \mu c_0)})\right)\right. \\ & \sqrt{b_0 \frac{-6b_0^4 - 12a_0^2 b_0^2 - \mu c_0 b_0^2 + 4\mu a_0^2 c_0 + \mu^2 c_0^2}{-c^2 b_0 + 2c\mu a_0^3 + 2cb_0^2 a_0 \mu + 4b_0^3 + 8b_0 a_0^2 + 2b_0 c_0 \mu}} \\ & \left. tanh\left(\sqrt{b_0 \frac{-6b_0^4 - 12a_0^2 b_0^2 - \mu c_0 b_0^2 + 4\mu a_0^2 c_0 + \mu^2 c_0^2}{-c^2 b_0 + 2c\mu a_0^3 + 2cb_0^2 a_0 \mu + 4b_0^3 + 8b_0 a_0^2 + 2b_0 c_0 \mu}}\ (x - ct)\right)\right], \end{aligned} \tag{28}$$

$$
\begin{aligned}
R(x,t) &= c_0 + \Bigg(\frac{24b_0^5 + 72b_0^3a_0^2 + 12b_0^3c_0\mu + 12a_0^2b_0c_0\mu - 3c^2b_0^3 + 18b_0^2ca_0^3\mu - 6a_0^2c^2b_0}{\mu ca_0(-3b_0^2 + \mu c_0)} \\
&\quad + \frac{6b_0^4a_0c\mu + 12a_0^5c\mu + 48a_0^4b_0 - c^2b_0\mu c_0 + 2c\mu^2a_0^3c_0 + 2cb_0^2\mu^2a_0c_0}{\mu ca_0(-3b_0^2 + \mu c_0)} \Bigg) \\
&\quad \Bigg\{ -\sqrt{\frac{b_0(-6b_0^4 - 12a_0^2b_0^2 - \mu c_0b_0^2 + 4\mu a_0^2c_0 + \mu^2c_0^2)}{-c^2b_0 + 2c\mu a_0^3 + 2cb_0^2a_0\mu + 4b_0^3 + 8b_0a_0^2 + 2b_0c_0\mu}} \\
&\quad tanh\Bigg(\sqrt{b_0\frac{-6b_0^4 - 12a_0^2b_0^2 - \mu c_0b_0^2 + 4\mu a_0^2c_0 + \mu^2c_0^2}{-c^2b_0 + 2c\mu a_0^3 + 2cb_0^2a_0\mu + 4b_0^3 + 8b_0a_0^2 + 2b_0c_0\mu}}\,(x - ct) \Bigg) \Bigg\}^{-1} \\
&\quad + \Bigg(2\frac{(-c^2b_0 + 2c\mu a_0^3 + 2cb_0^2\mu a_0 + 4b_0^3 + 8b_0a_0^2 + 2b_0c_0\mu)(a_0^2 + b_0^2)}{ca_0(-3b_0^2 + \mu c_0)} \Bigg) \\
&\quad \Bigg\{ -\sqrt{\frac{b_0(-6b_0^4 - 12a_0^2b_0^2 - \mu c_0b_0^2 + 4\mu a_0^2c_0 + \mu^2c_0^2)}{-c^2b_0 + 2c\mu a_0^3 + 2cb_0^2a_0\mu + 4b_0^3 + 8b_0a_0^2 + 2b_0c_0\mu}} \\
&\quad tanh\Bigg(\sqrt{\frac{b_0(-6b_0^4 - 12a_0^2b_0^2 - \mu c_0b_0^2 + 4\mu a_0^2c_0 + \mu^2c_0^2)}{-c^2b_0 + 2c\mu a_0^3 + 2cb_0^2a_0\mu + 4b_0^3 + 8b_0a_0^2 + 2b_0c_0\mu}}\,(x - ct) \Bigg) \Bigg\}^{-2} \qquad (29)
\end{aligned}
$$

More interestingly again the solution Eq. (28) exhibits shape changing property for the choices of parameters $a_0 = b_0 = c_0 = 1.1;\ c = 0.0004$. From the plots in Figs.(4a-d), one can infer that when $\mu = 0.5$, the solution suffers with multiple-periodic line solitonic oscillations. When the value of the strength of nonlocal term increases much and much further leading to the shape of anti-soliton at $\mu = 3.4$. A close inspection on the contour plots as presented in Figs.(4e-h) reveals that the stripes represent the peaks of the soliton and ultimately leading to a single peak with the higher amplitude tails. In a similar manner, the solution for $R(x,t)$ from Eq.(29) is also portrayed in Figs. (4i-l) for the choice of $a_0 = b_0 = c = 0.1$ and $c_0 = 0.2$ and it is evident that in this case the shape changing occurs from anti-soliton to anti-kink like director oscillations. From the contours depicted in Figs. (4m-p), it is clear that the gradient amplitude distribution at Fig. 4m leads gradually to the exact anti-kink with two distinguished maximum and minimum amplitude regions as depicted in Fig. 4p. From this study, one can conclude that the nonlocality arising from the long-range molecular interactions characteristic of NLC media could favour shape changing molecular deformations. This shape changing molecular deformations has also been reported by Srivasta et al with a different model of study [42]. Recently, Conti et al. [4] have presented the theory of spatial solitary waves in nonlocal NL media and reported self-trapping of light. The same has been predicted in nematic media, where the reorientation nonlinearity is saturable and nonlocal, it generallly stabilizes self focusing and creation of robust spatial soltions [43]. In a different context, it has been demonstrated that the spin soliton representing the dynamics of ferromagnetic spin chain admits shape changing during its evolution. This shape changing property can be exploited to reverse the magnetization without lost of energy which may have potential applications in magnetic memory and recording devices [44-45].

Solution (iv)

In a similar way, we compute another set of solutions for b, a_1, c_1, e_1, e_2 as follows

$$b = \frac{-b_0(-2b_0^2 + c_0\mu)(2b_0^2 + 4a_0^2 + \mu c_0)}{-c^2b_0 + 2c\mu a_0^3 + 2cb_0^2\mu a_0 + 4b_0^3 + 8b_0a_0^2 + 2b_0c_0\mu}, \tag{30a}$$

$$a_1 = -\frac{-c^2b_0 + 2c\mu a_0^3 + 2cb_0^2\mu a_0 + 4b_0^3 + 8b_0a_0^2 + 2\mu c_0}{c(-2b_0^2 + \mu c_0)}, \tag{30b}$$

$$c_1 = -\frac{b_0(-c^2b_0 + 2c\mu a_0^3 + 2cb_0^2\mu a_0 + 4b_0^3 + 8b_0a_0^2 + 2b_0\mu c_0)}{c(-2b_0^2 + \mu c_0)a_0}, \tag{30c}$$

$$\begin{aligned} e_1 = {} & \frac{24b_0^5 + 72b_0^3a_0^2 + 12\mu c_0b_0a_0^2 - 6a_0^2c^2b_0 + 12a_0^5c\mu + 20b_0^2ca_0^3\mu + 48a_0^4b_0 - 4c^2b_0^3}{a_0\mu c(-2b_0^2 + \mu c_0)} \\ & + \frac{8b_0^4ca_0\mu + 12b_0^3c_0\mu - c^2b_0c_0\mu + 2c\mu^2a_0^3c_0 + 2cb_0^2\mu^2a_0c_0}{a_0\mu c(-2b_0^2 + \mu c_0)}, \end{aligned} \tag{30d}$$

$$e_2 = \frac{2(-c^2b_0 + 2ca_0^3\mu + 2cb_0^2a_0\mu + 4b_0^3 + 8b_0a_0^2 + 2b_0\mu c_0)(a_0^2 + b_0^2)}{c(-2b_0^2 + \mu c_0)a_0}, \tag{30e}$$

Upon substituting Eqs. (30) in Eq. (12), the solution takes the following form

$$\begin{aligned} \psi(x,t) = {} & a_0 + \frac{-c^2b_0 + 2c\mu a_0^3 + 2cb_0^2\mu a_0 + 4b_0^3 + 8b_0a_0^2 + 2\mu c_0}{c(-2b_0^2 + \mu c_0)} \\ & \sqrt{\frac{b_0(-2b_0^2 + c_0\mu)(2b_0^2 + 4a_0^2 + \mu c_0)}{-c^2b_0 + 2c\mu a_0^3 + 2cb_0^2\mu a_0 + 4b_0^3 + 8b_0a_0^2 + 2b_0c_0\mu}} \\ & tanh\left(\sqrt{\frac{b_0(-2b_0^2 + c_0\mu)(2b_0^2 + 4a_0^2 + \mu c_0)}{-c^2b_0 + 2c\mu a_0^3 + 2cb_0^2\mu a_0 + 4b_0^3 + 8b_0a_0^2 + 2b_0c_0\mu}}\ (x - ct)\right) \\ & + \mathrm{i}\left[b_0 + \left(\frac{b_0(-c^2b_0 + 2c\mu a_0^3 + 2cb_0^2\mu a_0 + 4b_0^3 + 8b_0a_0^2 + 2b_0\mu c_0)}{ca_0(-2b_0^2 + \mu c_0)}\right)\right. \\ & \sqrt{\frac{b_0(-2b_0^2 + c_0\mu)(2b_0^2 + 4a_0^2 + \mu c_0)}{-c^2b_0 + 2c\mu a_0^3 + 2cb_0^2\mu a_0 + 4b_0^3 + 8b_0a_0^2 + 2b_0c_0\mu}} \\ & \left. tanh\left(\sqrt{\frac{b_0(-2b_0^2 + c_0\mu)(2b_0^2 + 4a_0^2 + \mu c_0)}{-c^2b_0 + 2c\mu a_0^3 + 2cb_0^2\mu a_0 + 4b_0^3 + 8b_0a_0^2 + 2b_0c_0\mu}}\ (x - ct)\right)\right], \end{aligned} \tag{31}$$

$$
\begin{aligned}
R(x,t) &= c_0+\left(\frac{24b_0^5+72b_0^3a_0^2+12\mu c_0b_0a_0^2-6a_0^2c^2b_0+12a_0^5c\mu+20b_0^2ca_0^3\mu+48a_0^4b_0-4c^2b_0^3}{a_0\mu c(-2b_0^2+\mu c_0)}\right.\\
&\left.+\frac{8b_0^4ca_0\mu+12b_0^3c_0\mu-c^2b_0c_0\mu+2c\mu^2a_0^3c_0+2cb_0^2\mu^2a_0c_0}{a_0\mu c(-2b_0^2+\mu c_0)}\right)\\
&\left\{-\sqrt{\frac{b_0(-2b_0^2+c_0\mu)(2b_0^2+4a_0^2+\mu c_0)}{-c^2b_0+2c\mu a_0^3+2cb_0^2\mu a_0+4b_0^3+8b_0a_0^2+2b_0c_0\mu}}\right.\\
&\left.tanh\left(\sqrt{\frac{b_0(-2b_0^2+c_0\mu)(2b_0^2+4a_0^2+\mu c_0)}{-c^2b_0+2c\mu a_0^3+2cb_0^2\mu a_0+4b_0^3+8b_0a_0^2+2b_0c_0\mu}}\;(x-ct)\right)\right\}^{-1}\\
&+\frac{2(-c^2b_0+2ca_0^3\mu+2cb_0^2a_0\mu+4b_0^3+8b_0a_0^2+2b_0\mu c_0)(a_0^2+b_0^2)}{c(-2b_0^2+\mu c_0)a_0}\\
&\left\{-\sqrt{\frac{b_0(-2b_0^2+c_0\mu)(2b_0^2+4a_0^2+\mu c_0)}{-c^2b_0+2c\mu a_0^3+2cb_0^2\mu a_0+4b_0^3+8b_0a_0^2+2b_0c_0\mu}}\right.\\
&\left.tanh\left(\sqrt{\frac{b_0(-2b_0^2+c_0\mu)(2b_0^2+4a_0^2+\mu c_0)}{-c^2b_0+2c\mu a_0^3+2cb_0^2\mu a_0+4b_0^3+8b_0a_0^2+2b_0c_0\mu}}\;(x-ct)\right)\right\}^{-2}. \qquad (32)
\end{aligned}
$$

In this case, the solution $\psi(x,t)$ as represented in Eq.(30), exhibits unusual breather like director oscillations which are both temporally and spatially periodic modes as depicted in Figs. (5a-c). As the value of μ increases the preiodicity becomes large leading to the reduction in the number of breathing modes can be seen more clearly in the corresponding contour plots. Eventually, the solution $R(x,t)$ in Eq.(32) is demonstrating the shape changing from antikink to antisoliton excitations which is not presented here.

4. Conclusions

The exact solitary wave solutions for the nonlocal Nonlinear Schrödinger equations governing the molecular deformations in NLC have been constructed using symbolic computation. As a physical relevance, the effect of nonlocal term on the solitary deformation profile leading to the shape changing property has been studied for different cases. The presented intriguing unifying shape changing character of the molecular deformations in NLC systems shines new light on self-localization in liquid crystals and may be exploited for NLC display devices. We believe that this will stimulate new experiments towards a deeper understanding of self-trapping and self-localization in highly nonlocal nonlinear NLC media and development of novel all-optical and switching devices.

Acknowledgments

The first author L.K. gratefully acknowledges the financial support from UGC in the form of major research project, BRNS, India in the form of Young Scientist Research Award and ICTP, Trieste, Italy in the form of Junior Associateship.

References

[1] P.G. de Gennes and J. Prost,**The Physics of Liquid Crystals**, Clarendon Press, Oxford (1993).

[2] S. Chandrasekhar, **Liquid Crystals**, Cambridge University Press, Cambridge (1992).

[3] L. Lam and J. Prost, editors **Solitons in Liquid Crystals**, Springer, New York (1992).

[4] C. Conti, M. Peccianti and G. Assanto, Phys. Rev. Lett. **91** (2003) 073901.

[5] L. Lam, Liq. Cryst. **14** (1993) 1873.

[6] L. Lin, in the proceedings of the conference on Statistcal Physics and Condensed Matter Theory, Wuhan (1981).

[7] G.Z. Zhu, Phys. Rev. Lett. **49** (1982) 1332.

[8] W. Helfrich, Phys. Rev. Lett. **21** (1968) 1518.

[9] L. Leger, Solid State Commun. **10** (1972) 697.

[10] K.B. Migler and R.B. Meyer, Phys. Rev. Lett. **66** (1991) 1485.

[11] L. Lin and C.Q. Shu, Acta Phys. Sin. **33** (1984) 165.

[12] L. Lin, C.Q. Shu and G. Xu Phys. Lett. **109A** (1985) 277.

[13] C.Q. Shu and L. Lin, Mol. Cryst. Liq. Cryst. **131** (1985) 47.

[14] L. Lam and C.Q. Shu, Bull. Am. Phys. Soc. **30** (1985) 328.

[15] A.L. Strinic, M. Petrovic, D.V. Timotijevic, N.B. Aleksic and M.R. Belic, Opt. Express. **17** (2009) 11698.

[16] M. Peccianti, I.B. Burgess, G. Assanto and R. Morandotti, Opt. Express. **18** (2010) 5934.

[17] M. Daniel, K. Gnanasekaran, Physica A **346** (2005) 250.

[18] M. Daniel, K. Gnanasekaran and L. Kavitha, Physica D **237** (2008) 3135.

[19] M. Daniel, K. Gnanasekaran, Phys. Lett. A **372** (2008) 2623.

[20] M. Daniel, K. Gnanasekaran, Physica A **346** (2005) 250.

[21] M. Simoes, Phys. Rev. E **56** (1997) 3061.

[22] J.R. Kelley and P. Palffy-Muhoray, Phys. Rev. E **55** (1997) 4378.

[23] M.A. Karpierz, Phys. Rev. E **66** (2002) 036603

[24] M. Lakshmanan, Phys. Lett. A **61** (1977) 53..

[25] L. Kavitha and M. Daniel, J. Phys. A. Math. Gen **36** (2003) 10471.

[26] L. Kavitha, P. Sathishkumar and D. Gopi, Phys. A. Math. Gen **43** (2010) 125201.

[27] N.R. Pereira and L. Stenflo, Phys. Fluids **20** (1977) 1733.

[28] D. Suter and T. Blasberg, Phys. Rev. A **48** (1993) 4583.

[29] J.P. Gordon, R.C.C. Leite, R.S. Moore, S.P.S. Porto, J.R. Whitney, J. Appl. Phys. **36** (1965) 3.

[30] M. Peccianti, G. Assanto, A. De Luca, C. Umeton and I.C. Khoo, Appl. Phys. Lett. **7** (2000) 77.

[31] H.L. Pecseli and J.J. Rasmussen, Plasma Phys. **22** (1980) 421.

[32] V.M. Perez-Garcia, V.V. Konotop and J.J. Garcia Ripoll, Phys. Rev. E **62** (2000) 4300.

[33] S. Abe and A. Ogura, Phys. Rev. E. **57** (1998) 6066.

[34] M.Wang, Phys. Lett. A **213** (1996) 279.

[35] E. Fan, Phys. Lett. A. **277** (2000) 212.

[36] W. Malfliet, Am. J. Phys. **60** (1992) 650.

[37] E. Fan, J. Phys. A **36** (2003) 7009.

[38] S.A. Elwakil, S.K. El. Labany, M.A. Zahran and R. Sabry, Phys. Lett. A **57** (2002) 179.

[39] M. Peccianti, C. Conti, G. Assanto, A. De Luca and C. Umeton, J. of Nonlinear Opt. Phys. **12** (2003) 525.

[40] G. Assanto, C. Conti and M. Peccianti, Int. Mod. Phys. Lett.B **18** (2004) 2819.

[41] G. Assanto, M. Peccianti and C. Conti, IEEE Journal of Selected Topics on Quantum Electronics **10** (2004) 862.

[42] S.K. Srivasta and G.S. Ranganath, Mol. Cryst. Liq. Cryst. **366** (2001) 337.

[43] A.W. Synder, D.J. Mitchell and Y.S. Kivshar, Mod. Phys. Lett B **9** (1995) 1479.

[44] L. Kavitha, P. Sathishkumar and D. Gopi, Phys. Scr. **79** (2009) 015402.

[45] M. Daniel and L. Kavitha, Phys. Rev. B **66** (2002) 184433.

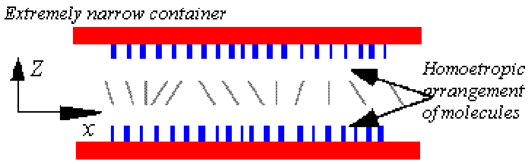

Figure 1: A sketch of the quasi one-dimensional nematic liquid crystal system contained in an extremely narrow infinite container.

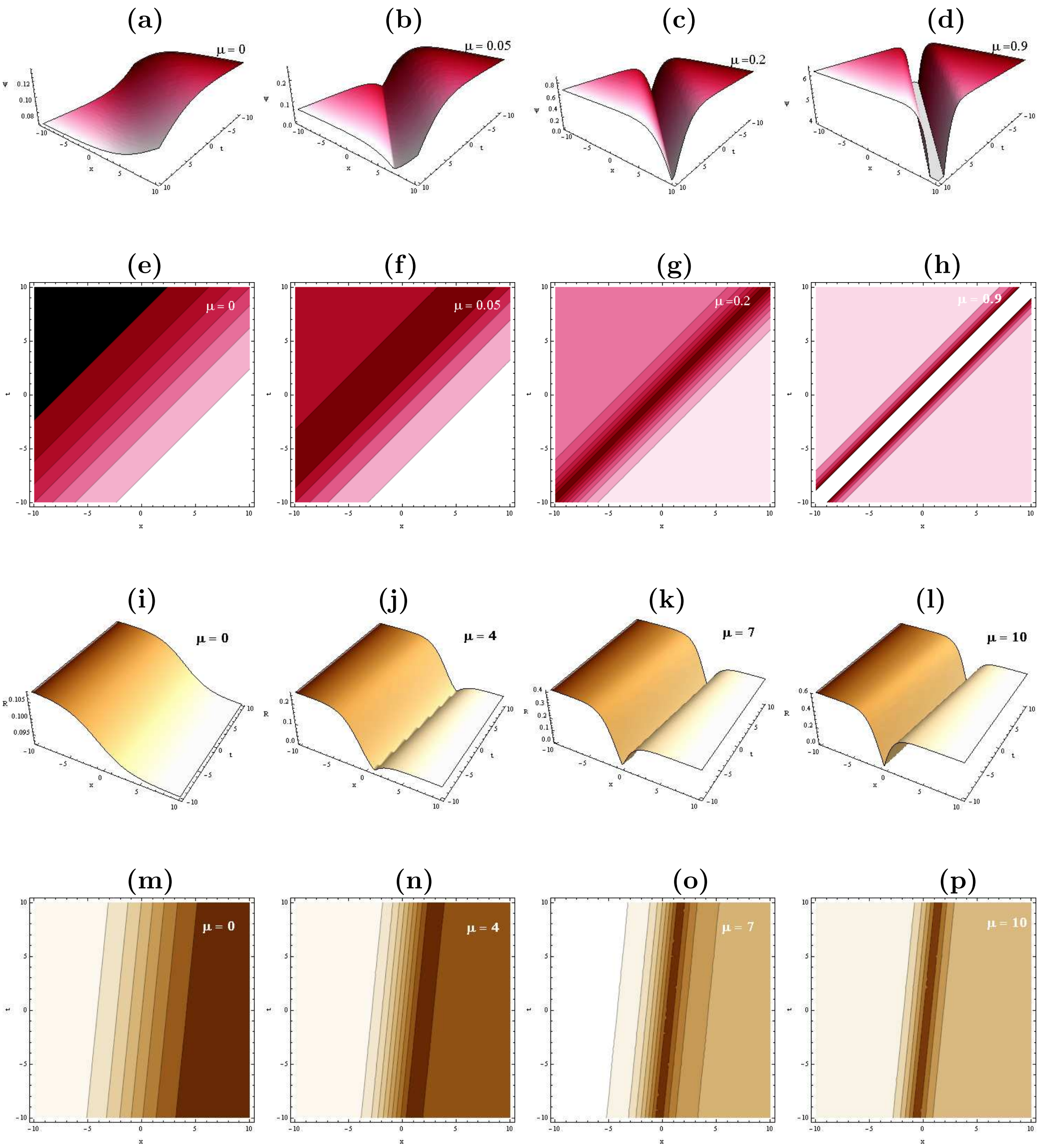

Figure 2: A snapshot of soltion changing shape from kink-anti-soliton (a-d), its contour plots(e-h) for Eq.(18) and anti-kink to anti-soliton (i-l) and its contour plots (m-p) for Eq. (19).

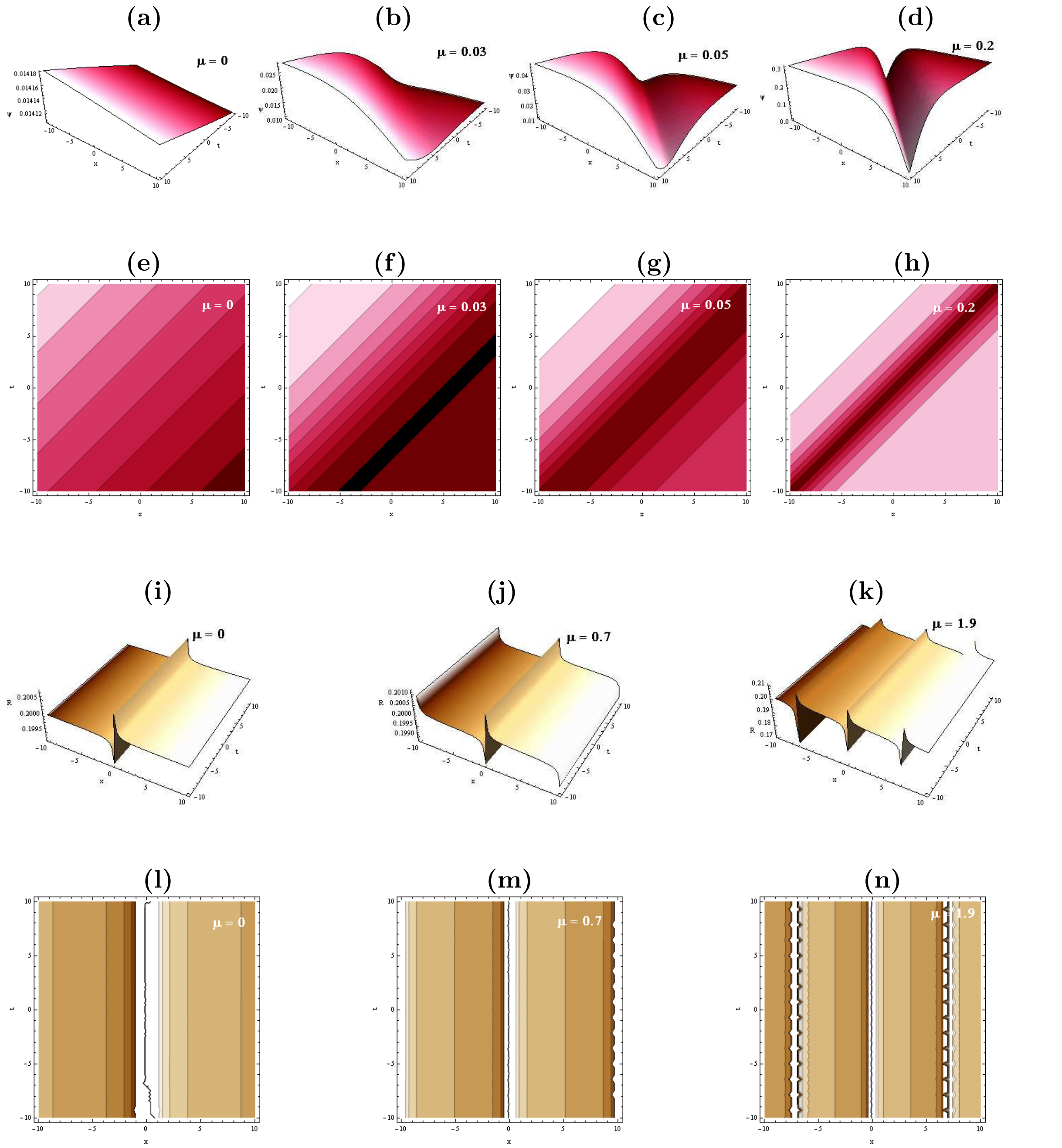

Figure 3: A snapshot of soltion changing shape from anti-kink to anti-soliton (a-d), its contour plots(e-h) for Eq.(21) and kink to multi-kink (j-k) and its contour plots (l-n) for Eq. (22).

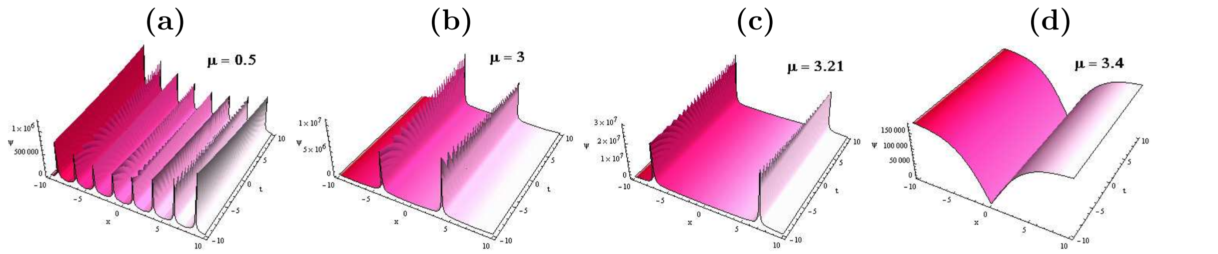

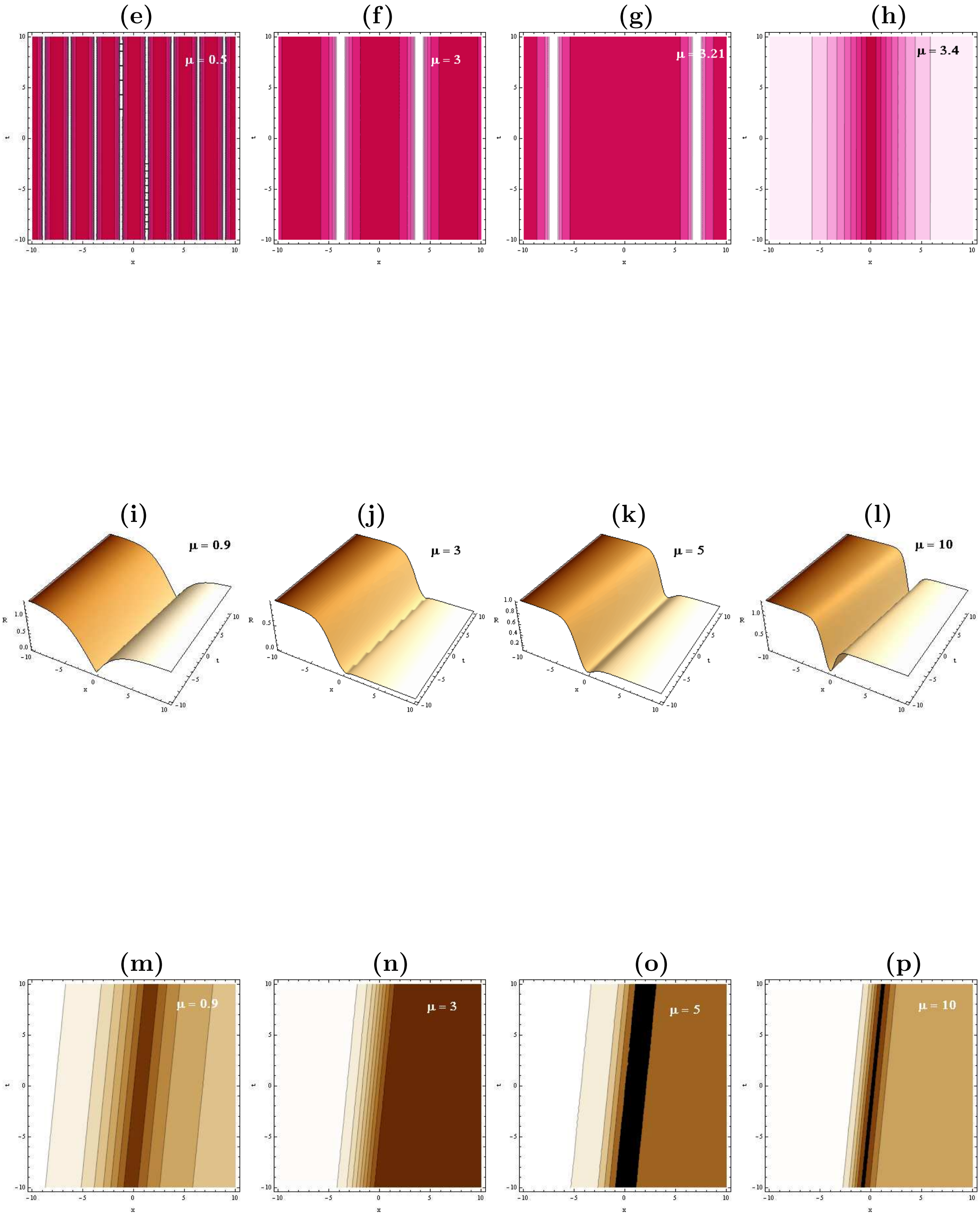

Figure 4: A snapshot of soltion changing shape from periodic line solitons to anti-soliton (a-d), its contour plots(e-h) for Eq.(28) and anti-kink to anti-soliton (i-l) and its contour plots (m-p) for Eq. (29).

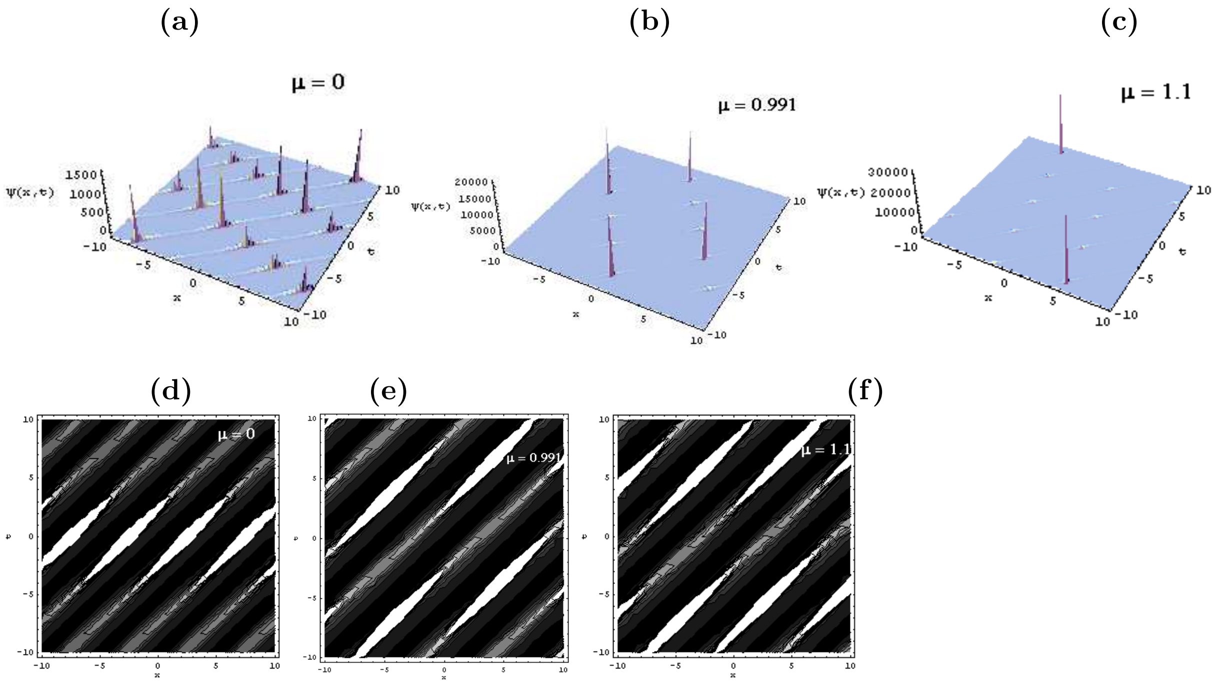

Figure 5: A snapshot of breathing soltion (a-c) and its contour plots(d-f) for Eq.(31)